PERGAMON

Quaternary Science Reviews 0 (2001) 1–18

QSR

Flow variability in the Scandinavian ice sheet: modelling the coupling between ice sheet flow and hydrology

Neil Arnold[a,*], Martin Sharp[b]

[a] *Scott Polar Research Institute, University of Cambridge, Lensfield Road, Cambridge, CB2 1ER, UK*
[b] *Department of Earth and Atmospheric Sciences, University of Alberta, Edmonton, AB, T6G 2E3, Canada*

Abstract

There is increasing geologic evidence for periodic flow variability within large ice sheets, manifested as spatially and temporally variable areas of fast ice flow, and resulting in the very complex patterns of lineations observed in formerly glaciated areas. However, many ice sheet models do not replicate this behaviour. A possible reason for this is that such models do not include a detailed treatment of basal hydrology. Changes in the character of sub-glacial drainage systems are believed to cause surges in valley glaciers. Recent ice sheet models, which have included basal hydrology or at least a link between basal velocity and the presence of water at the bed, often show flow variability. However, these models have typically assumed a deformable bed, or have made no assumptions about the nature of the bed. Whilst these assumptions seem applicable to areas close to the former margins of Quaternary ice sheets, they are less applicable to interior areas. These areas typically show thin or scanty till cover over eroded bedrock, and the presence of eskers, which are indicative of drainage in sub-glacial tunnels. We have developed a two-dimensional time-dependent ice sheet model that includes hard-bed basal hydrology. This allows calculation of sub-glacial water pressures and the use of a water pressure dependent sliding law to calculate ice sheet velocities. When used to simulate the Weichselian Scandinavian ice sheet, with late Quaternary climate and sea level as forcing functions, this model develops localised areas of fast-flowing ice, which vary in extent and in distance of penetration into the interior of the ice sheet both spatially and temporally. The behaviour of these lobes depends crucially on the influence of the evolving ice sheet topography on the routing of subglacial water flow, due to the resulting variations in the subglacial hydraulic potential which drive the water flow. Bedrock topography also has some influence, but fast flow areas are not confined to obvious topographic troughs. A relatively thin ice sheet with low surface slopes is produced in areas experiencing fast ice flow. Generally, two to four separate areas of fast flow can be recognised, and these are similar in size and shape to the 'lobes' identified in some geologically based reconstructions of the Scandinavian ice sheet. Within the fast-flowing areas, sub-glacial drainage is typically in a cavity-based system. However, tunnel-based drainage is predicted to have extended up to 150 km from the ice sheet margin, particularly during deglaciation. Because of the changes in ice sheet topography associated with fast flow, and the resulting changes in the pattern of sub-glacial water flow, the model predicts that these fast-flowing lobes interacted in complex ways, and exhibited quasi-periodic switching between fast and slow flow. © 2001 Published by Elsevier Science Ltd.

1. Introduction

There is increasing geologic evidence that large Quaternary ice sheets experienced periodic, internally driven oscillations. Such evidence includes so-called "Heinrich layers" in Atlantic marine sediments (Bond et al., 1992), and geomorphic evidence for localised fast flow within ice sheets. This is indicated by low gradient ice surface profiles (Mathews, 1974), localised long distance erratic transport and debris dispersal (Dyke and Morris, 1988), and "surge moraines" defining former ice sheet margin positions (Dyke and Prest, 1987). In Scandinavia, Punkari (1984) described the episodic formation of up to 8 ice lobes during the last deglaciation and suggested that these consisted of 100–200 km wide areas of fast-flowing ice bordered by areas of more slowly moving ice.

Large-scale studies in both North America and Scandinavia, based on satellite imagery (e.g. Punkari, 1989; Boulton and Clark, 1990a, b; Clark, 1993; Boulton et al., 2001) or comprehensive compilations of geologic and geomorphic evidence (e.g. Kleman et al., 1997), also indicate a high degree of flow variability within large mid-latitude ice sheets during the Weichselian. The studies by Klemans et al. and Boulton et al. in particular make ambitious reconstructions of ice extent and

*Corresponding author. Tel.: +44-1223-336-540; fax: +44-1223-336-572.
E-mail address: nsa12@cus.cam.ac.uk (N. Arnold).

PII: S 0 2 7 7 - 3 7 9 1 (0 1) 0 0 0 5 9 - 2

dynamics for the whole of the last glacial cycle. These studies conclude that the Scandinavian Ice Sheet exhibited complex patterns of flow variability during both glacial advance and retreat phases. Part of this complexity seemed to be due by the migration of the ice divide in response to climate change, but it also seemed to be due to the spatial and temporal variability of fast flowing areas of the ice sheet.

The high degree of flow variability implied by such studies is probably linked to changes in the nature of the bed of the ice sheet. Such changes could include a shift between frozen and thawed bed conditions, or a change in ambient water pressure conditions over a thawed bed. It could also include a switch between hard and soft bed conditions, although the occurrence of bed deformation is dependent not only upon the existence of sub-glacial sediment, but also upon the ambient water pressure. The occurrence of high water pressure is critical, as it allows rapid basal motion by sliding (Iken, 1981), deformation of weak sub-glacial sediments (Boulton and Hindmarsh, 1987), or some combination of these processes (Iverson et al., 1995).

Many numerical ice sheet models have either neglected basal sliding or treated basal hydrology in only a simple way. As a result, they have not simulated spatially localised and temporally oscillatory fast flow (e.g. Huybrechts, 1992; Lindstrom, 1990). More recently, however, Payne (1995) found that a two-dimensional, thermomechanical flowline model, in which basal sliding was possible only where the bed of the ice sheet was at the pressure melting point, exhibited periodic oscillations. The area experiencing fast flow expanded headwards from the margin of the ice sheet, until the ice sheet thinned and flattened sufficiently that fethe bed re-froze and fast flow stopped. In a three-dimensional model, this instability was manifest as spatially discrete, but temporally stable, areas of fast flow, apparently analogous to ice streams (Payne and Dongelmans, 1997). In an application of this model to the West Antarctic Ice Sheet, Payne (1998, 1999) produced similar flow features. In this case, however, the Siple Coast ice streams (in particular Ice Streams A, B, and C) interacted with each other via an ‘ice capture’ mechanism, which resulted in quasi-periodic flow variability. In these studies, a melting bed is a sufficient condition for fast flow, and there is no treatment of the basal hydrological system. This is significant because it is widely believed that the configuration of the sub-glacial drainage system can exert considerable influence on basal motion through the effect of the sub-glacial water pressure on rates of sliding and/or bed deformation (e.g. Iken, 1981; Kamb, 1987; Fowler, 1987a, b).

In a separate modelling development, Fowler and co-workers (Fowler and Johnson, 1995, 1996; Fowler and Schiavi, 1998) have produced a model to evaluate ‘surging’ by ice sheets, in which a melting bed is only a necessary condition that allows basal motion. The nature of the hydrological system also plays a fundamental role. These models specifically include a treatment of the basal hydrology, and its influence on basal movement (however caused), and allow fast ice flow only when the bed is melting and sub-glacial water pressures are high. Fowler and co-workers find that a ‘hydraulic runaway’ exists in these models. Basal sliding is initiated when the bed reaches the melting point, and increases frictional heating of the bed. This increases water discharge, which for the hydrological configuration they envisage, leads to an increase in water pressure, and hence to an increase in sliding velocity, and higher frictional heating. This cycle is broken when the bed eventually re-freezes as a result of rapid thinning of the ice. The models used in these studies are zero- or one-dimensional, and cannot predict the spatial manifestation of such surges. However, Fowler and co-workers suggest that for unconfined, two-dimensional flow, the instability may manifest itself as spatially discrete areas of fast flow, rather than as temporal switching (Fowler and Johnson, 1995; Fowler and Schiavi, 1998).

Fowler’s models assume some form of ‘soft’ bed condition, with basal motion controlled by sediment deformation. For these conditions, basal water pressure increases with water discharge, regardless of whether the water flows in a patchy film at the ice/bed interface (Alley, 1989), or in ‘canals’ incised into the till surface (Walder and Fowler, 1994). Such conditions are probably found beneath the present-day West Antarctic ice streams (Engelhardt and Kamb, 1997), although even in these conditions, there is evidence that basal sliding (or deformation of a very thin layer at the ice/till interface, rather than pervasive till deformation) accounts for the bulk of ice stream velocity (Engelhardt and Kamb, 1998). These ‘soft’ bed conditions may also have occurred in some areas overlain by Quaternary ice sheets at or near their maximum extent. However, they probably did not occur beneath the interior regions of such ice sheets, where the beds are generally of exposed bedrock, with a thin, discontinuous till cover. Nevertheless, these areas show geomorphic evidence for fast ice flow (as discussed above). They are also characterised by the presence of eskers, which suggests that the hydrological configuration beneath these areas may have been very different (Clark and Walder, 1992). This is significant because, under steady state conditions at least, tunnel-based drainage systems are associated with an inverse relationship between water pressure and discharge (Röthlisberger, 1972).

A separate problem here is the possible role played by the drainage of subglacial water in groundwater aquifers. In a series of one-dimensional model-based studies of groundwater flow, Boulton and co-workers (Boulton et al., 1995; Boulton and Caban, 1995) have argued that for marginal areas of the Scandinavian ice sheet, underlain by Mezozoic and Cenozoic sedimentary rocks, the permeability of these beds is sufficient to drain meltwater beneath the ice sheet without the need for a hydrological system at the ice/bed interface. Thus, effective pressures in their model are high, suggesting basal hydrology has limited impact on ice dynamics (although ice dynamics are not explicitly modelled in their studies). This is seemingly contrary to most geological evidence, however, so they suggest that drainage through an overlying clay stratum (ignored in their studies) could produce a large drop in hydraulic potential across it, allowing low enough effective pressures at the upper surface of the layer to permit shear deformation. On the central shield areas of Scandinavia, however, bedrock permeablities are insufficient to drain meltwater, implying some form of hydrological system must occur at the ice-bed interface. The presence of eskers in these areas would seem to support this conclusion, and imply that the nature of the subglacial drainage system could affect ice sheet dynamics.

Boulton and co-workers assume that only water produced by basal melting will be present at the ice-bed interface. As discussed below, however, in this study we investigate the effects of allowing surface meltwater to reach the bed in certain circumstances. Surface melting is typically one to four orders of magnitude larger than basal melting (e.g. Boulton et al., 1995), and if such melt did reach the bed, it might supply sufficient water to require drainage at the ice-bed interface, even on the Mesozoic and Cenozoic aquifiers. This would seem to provide an alternative solution to the problem of high effective pressures in these marginal areas in the reconstructions by Boulton et al. (1995) and Boulton and Caban (1995), as the basal hydrological system itself would determine effective pressure, rather than the transmissibility of the underlying aquifiers.

Model-based studies of the Scandinavian ice sheet have adopted a variety of solutions to the problem of the apparent flow variability within this ice sheet. Early studies, in common with most ice sheet models, ignored the problem, leading to similar reconstructions to the CLIMAP study (Denton and Hughes, 1981), with large, thick, and quite static ice sheets. Other models have sought to allow fast sliding in particular areas of the ice sheet, and then examine its impact. These areas have often been chosen on the basis of geological evidence, and then imposed in the ice sheet model as a different basal boundary condition (e.g. Holmlund and Fastook, 1993). Whilst this may allow the impact of particular areas of fast flow on the ice sheet dynamics to be evaluated, it does not allow the apparent variability of fast flow to be simulated, and nor does it address the question of why fast flow develops in particular areas, and not others, in the first place. A recent study by Payne and Baldwin (1999) acknowledges these problems, but adopts a different approach. They use a three-dimensional thermo-mechanical model, but neglect basal movement, instead concentrating on the strong dependence of ice viscosity on basal temperature, and the effect this has on ice dynamics under a steady climate. This paper does not attempt to produce a 'geologically realistic' reconstruction; rather, it seeks to explore the dynamic behaviour of an appropriately sized model ice sheet on a realistic topography, under certain conditions. This model develops discrete areas of faster flow around the margins, which match well with geological evidence, and which occur due to the feedback between basal temperature and deformation velocity; warmer ice leads to fast flow, which lowers ice surface elevation, leading to fast flow due to the concentration of ice discharge (and hence heat production) in the faster flowing areas.

In this paper, we adopt a similar philospohy to this latter study. We do not seek to develop a 'realistic' model of the Scandinavian Ice Sheet, but rather we focus on the potential impact of basal hydrology on ice sheet dynamics, through the possible feedbacks between the resulting ice sheet topography, flow and hydrology. We apply the model, with variable climate and mass balance parameters adjusted to give a realistically sized ice sheet at the LGM, on a realistic topography, using the Late Weichselian Scandinavian ice sheet as an example. The model presented here follows those of Fowler and co-workers by treating a melting bed as only a necessary condition for fast flow; low effective pressure must also be present if fast flow is to occur. The basal hydrological system is therefore modelled directly, and allowed to exist in either of two possible states; a 'distributed', cavity-based system, in which water pressure changes directly with water discharge (Kamb, 1987; Fowler, 1987a), or a tunnel-based system, with an inverse water pressure/discharge relationship. The transition between these two states is controlled using a stability criterion for tunnel-based flow (Fowler, 1987a, b). Basally produced meltwater and, under certain circumstances, surface meltwater supply the basal hydrological system. However, following the work of Payne and co-workers, the model has two spatial dimensions, and thus allows the impact of drainage system behaviour on the spatial and temporal variability of ice sheet flow to be evaluated. Our aim is to investigate how the dynamics of the model ice sheet are affected by the inclusion of a physically based model of sub-glacial hydrology. In particular, we are interested in whether the inclusion of such a model can lead to the degree of spatial and temporal flow variability that the geological record suggests, and which has generally not been captured by ice sheet models to date.

2. Model formulation

The model used in this study is a two-dimensional version of that used by Arnold and Sharp (1992) to investigate the influence of changing sub-glacial hydrology on the dynamics of the late Weichselian Scandinavian ice sheet. Full details are given in the Appendix A, but we summarise the main features of the model here. It is based on a time-dependent mass continuity equation, solved using a semi-implicit, alternating direction, finite difference scheme. It simulates the time-dependent evolution of ice sheet form and flow. Ice is assumed to deform by simple shear, and sliding occurs where the base of the ice is calculated to be at the pressure melting point. A simple scheme, which compares heat produced at the base of the ice sheet (by geothermal and frictional heating) with the temperature gradient needed to conduct that heat away from the bed, is used to determine whether the glacier bed is at the pressure melting point (Arnold and Sharp, 1992). Any excess heat, which would raise the temperature above the pressure melting point, is assumed instead to melt basal ice. The resulting water then enters the modelled sub-glacial drainage system. This thermal scheme is very similar to that adopted by Fowler and co-workers (Fowler and Johnson, 1995, 1996; Fowler and Schiavi, 1998), who assume that all heat produced by ice movement is produced in a boundary layer at the bed of the ice mass, in which the majority of shear occurs. This scheme therefore neglects the possible effects on basal temperatures of advection of cold ice from areas upstream or adjacent to areas in which fast flow occurs. However, in a two-dimensional flow-line study, Payne (1995) found that, even at some distance from the ice sheet margins, the advection of cold ice formed a minor component of the heat budget and had little effect on the basal temperature. This scheme also allows for effectively instantaneous transmission of surface temperature changes to the bed. Timescales of temperature diffusion in ice sheets can be approximated by dividing the ice thickness by the depth averaged vertical velocity, which can be taken to be half the accumulation rate (Paterson, 1994, p. 338). At the divide at the LGM, modelled ice thicknesses are 2000–2500 m, and accumulation rates are ~ 0.2–$0.3\,\mathrm{m\,a^{-1}}$, giving a response time of 15,000–25,000 years. Nearer the ice sheet margins, or during deglaciation, thicknesses of ~ 1000 m and accumulation rates of $\sim 0.5\,\mathrm{m\,a^{-1}}$ give response times of ~ 4000 years. We simulate this delay, and explore the model sensitivity to changing surface temperatures by 'lagging' the climatically induced surface temperature changes used in the calculations of basal temperature by a variable amount between 1000 and 20,000 years in some model runs.

The sliding relationship used (McInnes and Budd, 1984) depends on both the local shear stresses, and the effective pressure (that is, the ice overburden pressure minus the subglacial water pressure). Since the effective pressure depends on the discharge in the sub-glacial drainage system, both the water inputs to this system, and the flow path followed by sub-glacial water must be known. There are two possible sources of water: basal melt and surface melt.

Evidence from esker sedimentology suggests that discharge in at least some sub-glacial tunnels varied on both diurnal (Allen, 1971) and annual (Banerjee and McDonald, 1975) time scales. Similarly, cyclic sequences in esker sediments have been linked to varved clays in pro-glacial lakes, which are demonstrably annual in origin (Kleman et al., 1997). This implies that surface-derived melt reached the ice sheet bed in some areas. For this to be possible, surface runoff must have penetrated significant thicknesses of ice at sub-freezing temperatures. Water draining into crevasses is a source of both sensible and frictional heat and, if discharge is sufficient, it may be capable of penetrating the subsurface cold layer and reaching ice at the pressure melting point below. Investigations of water flow, moulin water pressures, and glacier velocity on White Glacier, Axel Heiberg Island, suggest that surface streams with discharges of 0.1–$0.2\,\mathrm{m^3\,s^{-1}}$ could penetrate to the glacier bed through up to 300 m of cold ice (Iken, 1974; Blatter, 1987). Another mechanism which might allow surface water to penetrate to the bed is the filling of surface crevasses by meltwater (Mavlyudov, 1995, 1998; Scambos et al., 2000). Scambos et al., in a study of the breakup of Antarctic ice shelves, argue that meltwater can keep existing crevasses open in areas unfavourable to crevasse development, and that the pressure exerted by the water can lead to downwards propagation of the crevasse through the entire ice thickness if the crevasses are deeper than a critical depth (determined by factors including the fracture toughness of ice, ice density and the degree of water filling). Calculated critical depths are generally smaller than 20 m. Although this study is based on floating ice shelves, the key assumptions would seem applicable to ice sheets, especially in areas of longitudinal extension, as at the head of areas of fast ice flow in ice sheets.

To simulate these possibilities, we assume that surface melt can reach the bed if (a) the surface water discharge in a given grid cell exceeds some critical value (Q_{crit}), and (b) the base of the ice sheet in the grid cell is at the pressure melting point. We calculate the surface water discharge by integrating surface ablation rates down the ice sheet surface. In any cell with a bed temperature at the PMP, where the surface water discharge exceeds Q_{crit}, this discharge is added to any basal melt. To allow for the large thicknesses of cold ice which surface runoff must penetrate to reach the bed of ice sheets, we use $10\,\mathrm{m^3\,s^{-1}}$ as an estimate of Q_{crit} in the 'standard run'. The penetration of surface melt through ice sheets has not been conclusively established, nor ruled out, so we investigate the impact of this assumption on basal hydrology and ice sheet flow dynamics by varying the value of Q_{crit} in a series of sensitivity analyses.

Once the quantities of basal melt, and surface melt which penetrate to the bed of the ice sheet, are known, these are integrated down the subglacial hydraulic potential surface (Shreve, 1972) to give the subglacial water discharge in each grid cell.

These calculations then allow the nature of the subglacial drainage system, and the resulting effective pressure to be calculated. Two possible configurations are allowed; a system of 'linked cavities' (Kamb, 1987), or a more efficient system of subglacial tunnels (Röthlisberger, 1972). Water pressures within these systems are calculated using the equations of Fowler (1987a, b). A stability criterion, following Fowler (1987a, b) is used to determine which type of drainage system dominates in each grid cell.

The model makes separate calculations of accumulation and ablation rates over the ice sheet. Precipitation rates across the study area at 120 ka BP were assumed to be the same as at the present day. This distribution was modelled using empirical relationships, which relate precipitation to latitude, longitude and elevation. During the model run, precipitation rates were altered as a function of the imposed temperature forcing and additional cooling associated with elevation changes induced by ice sheet growth and decay. These relationships to do not account for possible changes of the atmospheric circulation that may have resulted from ice sheet growth and decay.

Ablation rates were calculated using the method of Budd and Smith (1981). The ablation rate is specified as a function of elevation relative to the elevation of the $1\,\mathrm{m\,a^{-1}}$ ablation contour (E_0), which is itself a function of latitude and the imposed temperature change, converted to an elevation change using a lapse rate of $6.5^{\circ}\mathrm{C\,km^{-1}}$. Calving rates at marine margins of the ice sheet were determined using a water depth dependent calving law (Brown et al., 1982). These relationships all have obvious limitations. However, there are still enormous uncertainties about the climate during the Last Glacial period. We therefore justify the use of these relationships on the grounds that our aim is to investigate how the dynamics of the model ice sheet are affected by the inclusion of a physically based model of sub-glacial hydrology. We emphasise that we have not tried to produce as 'geologically realistic' a simulation of the ice sheet as possible.

Ice sheets exert a profound effect on bedrock topography through the process of isostasy. A variety of earth-models have been used in conjunction with ice sheet models to account for this effect (e.g. Le Meur and Huybrechts, 1996). However, many of the more physically realistic schemes have the disadvantage that many parameter values needed are subject to a high degree of uncertainty. This can make within-model variations due to parameter uncertainties of the order of between-model variation due to model formulation (Le Meur and Huybrechts, 1996). Given these problems, and the aims of this study, we adopt a simple diffusion-based scheme to calculate the isostatic response to the growth and decay of the ice sheet.

3. Model inputs

The model requires two main input data sets; a Digital Elevation Model of the bedrock topography in the study area, and the forcing functions used to drive the model. The study area (Fig. 1) extends from approximately 50°N 2°E to 75°N 50°E, and includes the whole of Scandinavia, the Baltic States and European Russia as far east as the Urals. The model uses a 40 km grid, which produced a 75 by 75 point DEM, using a Lambert conformal conic projection. At the start of a run (120 ka BP) the area is assumed to be ice free, and bedrock topography is assumed to be in isostatic equilibrium.

Forcing functions used to drive the model are eustatic sea level, taken from Shackleton (1987), and climatic change. The Laurentide ice sheet makes by far the largest contribution to eustatic sea level change, with the Scandinavian ice sheet responsible for perhaps 15–18 m out of a total change of c. 120 m at the LGM (Lambeck et al., 1998). We therefore treat eustatic sea level as an

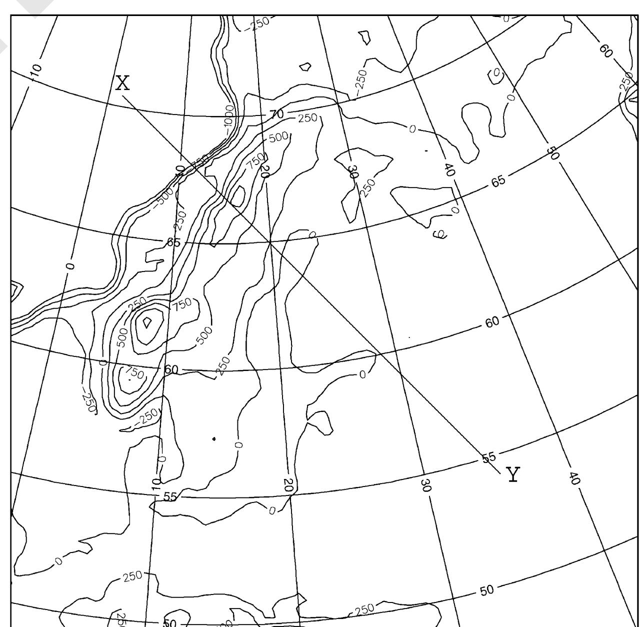

Fig. 1. Bedrock topography of the study area. Contours in m above sea level.

external variable. The GRIP δ^{18}O record (Johnsen et al., 1992; Dansgaard et al., 1993) was converted into an inferred temperature history using the conversion factor of 0.62 δ^{18}O K^{-1} (Dansgaard et al., 1973) and used as the climatic forcing for the model. Although this is a very simple system, we justify it given our aims, which are to investigate the role of basal hydrology on ice sheet dynamics.

4. Results of the standard model

For these runs, the model is run from 120 ka BP to the present day. However, we focus the discussion on the Late Weichselian period, as geological evidence for the behaviour of the ice sheet is most plentiful for this time, and the larger ice sheet makes the impact of the changing ice sheet hydrology on the ice sheet behaviour more obvious. In the following discussion, the reference to periods and localities is for descriptive purposes only; we make no claims that the model is accurately predicting the occurrence of fast flow in particular times or places. We compare the behaviour of the model ice sheet with geological evidence in only in a qualitative sense. We are interested in whether the dynamic behaviour of the model and the nature of the hydrological system predicted are comparable with those inferred from geological evidence, rather than in exact spatial and temporal matches between the model and geological reconstructions.

As the model ice sheet grows towards its maximum extent, it develops unusual surface forms (Fig. 2), with distinct areas of the ice sheet showing convex-out lower elevation contours, but concave-out mid-elevation contours, which we call 'lobes'. Such a lobe is always present over parts of southern Norway and Sweden (Location A in Fig. 2), in the south-western part of the ice sheet, but patterns of lobe development along the southern and eastern margins of the ice sheet vary over time. At 22,000 model years BP (Fig. 2a), there is a lobe over the Baltic Sea (Location B). At 18,000 model years BP (Fig. 2b), however, lobate areas occur on the eastern margins of the ice sheet over Finland and the Baltic States (Location C), rather than over the Baltic Sea. The lobes have narrow heads and became wider downstream. This configuration is similar to that of the lobes in the geologically based reconstructions of Punkari (1984), and to the 'surge fans' described by Kleman et al. (1997), although the model lobes can become very broad.

Throughout the period 22,000 model years BP to 18,000 model years BP, the ice divide shows a strong eastward convexity, caused by strong west or north-west ice flow over the lowest part of the Scandinavian mountain chain in central Norway, in broad agreement with Kleman et al. (1997). During ice sheet growth, the

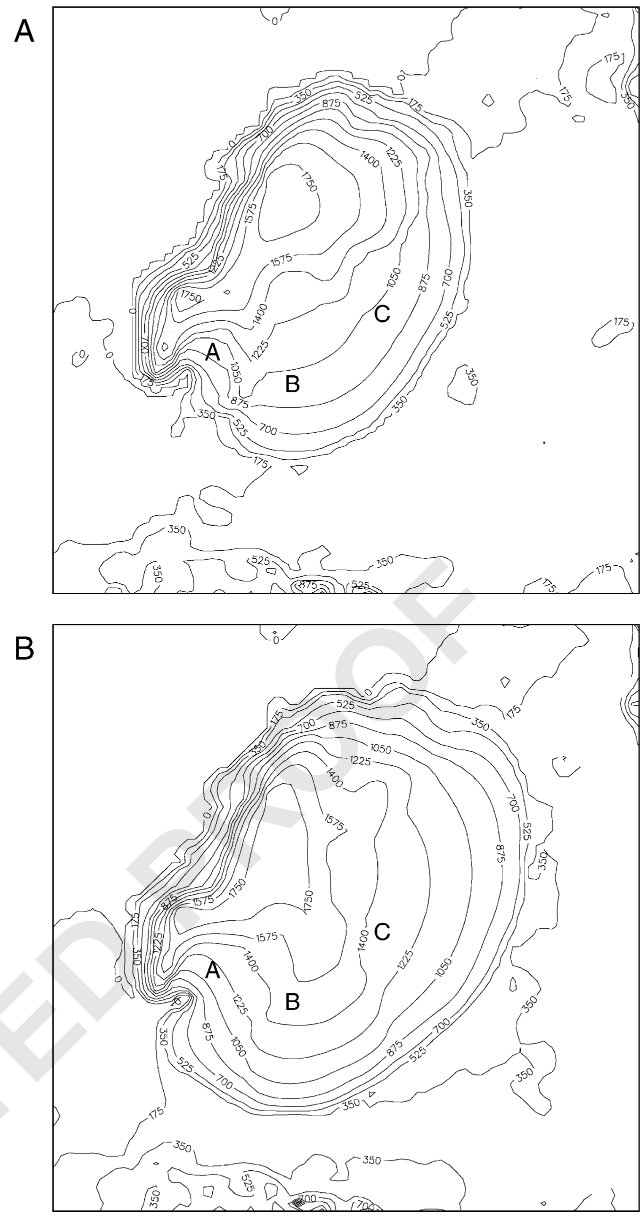

Fig. 2. Ice sheet (and surrounding topography) surface elevation. (a): At 22,000 yrs BP; (b): at 18,000 yrs BP. Contours in metres above contemporaneous sea level. For locations see text. X–Y denotes transect used in Figs. 7 and 9.

ice divide does not migrate very far to the east. It reaches the present-day western shore of the Gulf of Bothnia or a little further east between around 22,000 model years BP and 16,000 model years BP, before retreating west. During this period, however, the exact divide location fluctuates in response to lobe development. Dome surface elevations are quite low, with a maximum of around 2000 m. The lobate flow pattern is clearly reflected in the ice sheet velocity field (Fig. 3a and b). Fast ice flow occurs throughout the period shown in Figs. 2 and 3 in the south west of the ice sheet (around the southern Norwegian/Swedish border, location A),

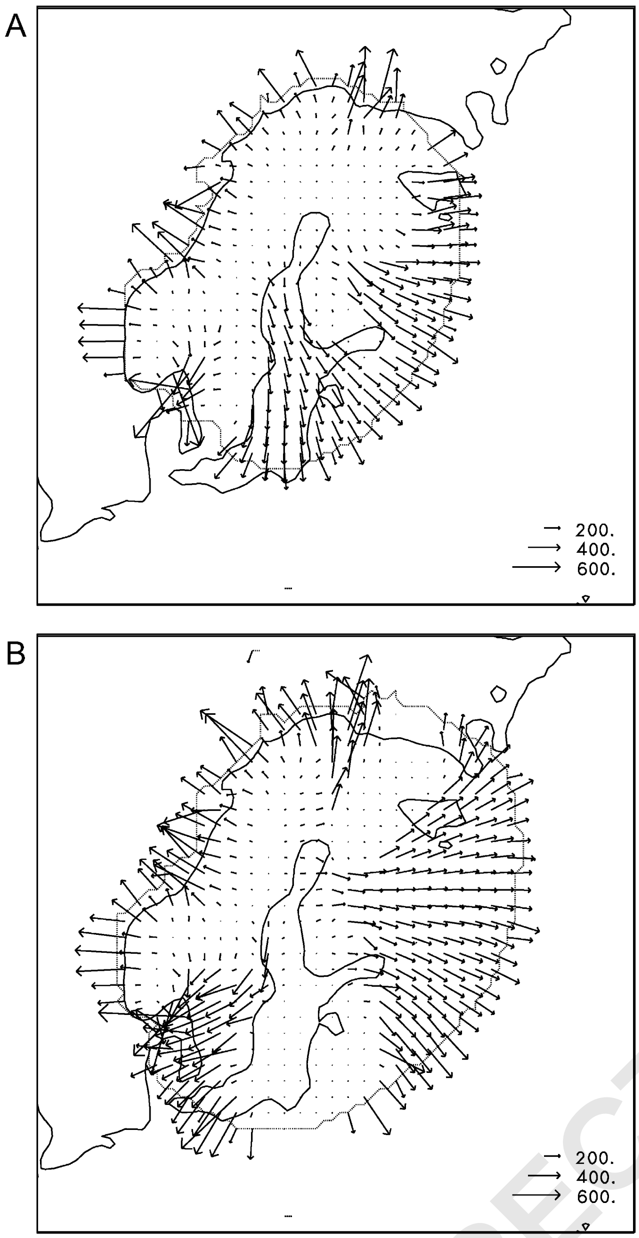

Fig. 3. Ice sheet velocity distribution. (a): At 22,000 yrs BP; (b): at 18,000 yrs BP. Values in m yr^{-1}.

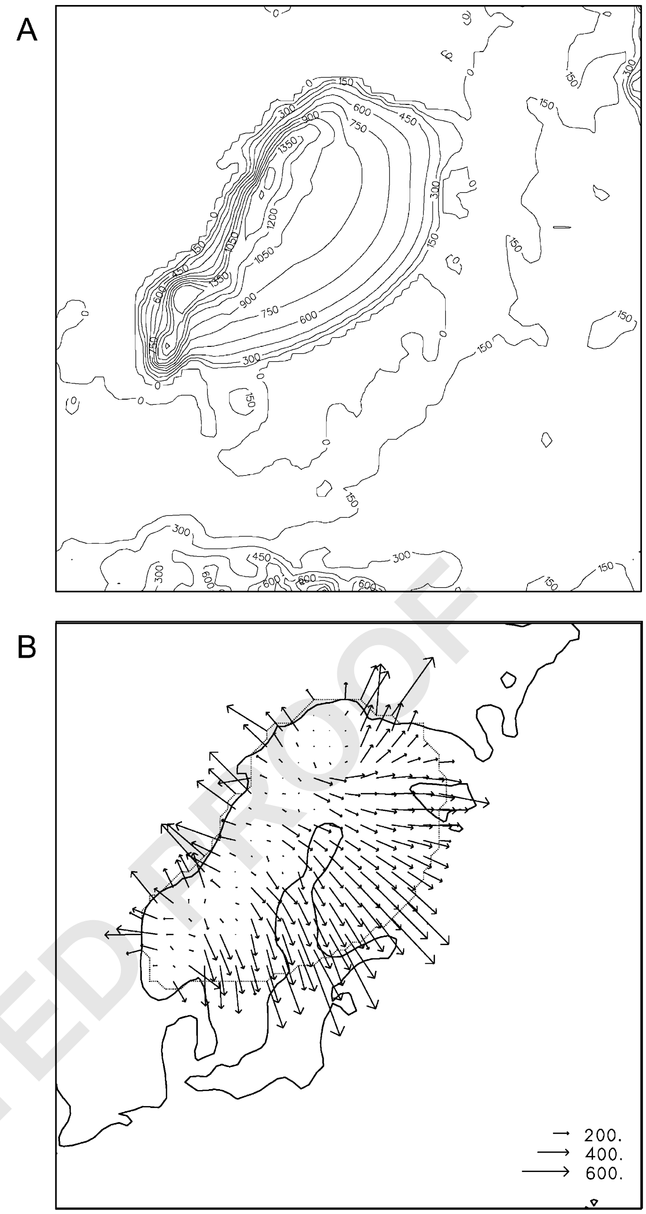

Fig. 4. Ice sheet configuration at 12,000 yrs BP. (a): Surface elevation, including surrounding topography (contours in metres); (b): velocity distribution (values in m yr^{-1}).

while changing patterns of fast flow occur on the southern (location B) and eastern margins (location C). Here, the areas of high velocity are associated with low surface slopes ($\sim$0.002–0.001, c.f. slopes for Siple Coast ice streams of $\sim$0.001 (Bentley, 1987)), while along the Norwegian margin of the ice sheet, and in the south west, high velocities occur in areas with steep surface slopes ($\sim$0.005–0.01, c.f. slopes for Lambert Glacier of $\sim$0.0075 (Bentley, 1987)).

After reaching its maximum areal extent at 16,300 model years BP (rather later than in many geological reconstructions), the ice sheet retreats rapidly. Fast ice flow transports large volumes of ice from the interior of the ice sheet to the ablating margins and lowers the elevation of the ice sheet surface. At 12,000 model years, BP (the equivalent of the Younger Dryas Stade), the topographic effect of the lobes has become less obvious, but the velocity field shows three to five distinct lobes along the eastern margin, with differing flow directions and source areas (Fig. 4). This pattern of flow is in close agreement with the reconstructed 'surge fans' for this period in this region proposed by Kleman et al. (1997).

Cold-based ice occurs in central regions of the model ice sheet, with warm-based ice in marginal areas. In the model, the cold-based area is quite extensive during glacial build-up, and at the maximum extent (Fig. 5a).

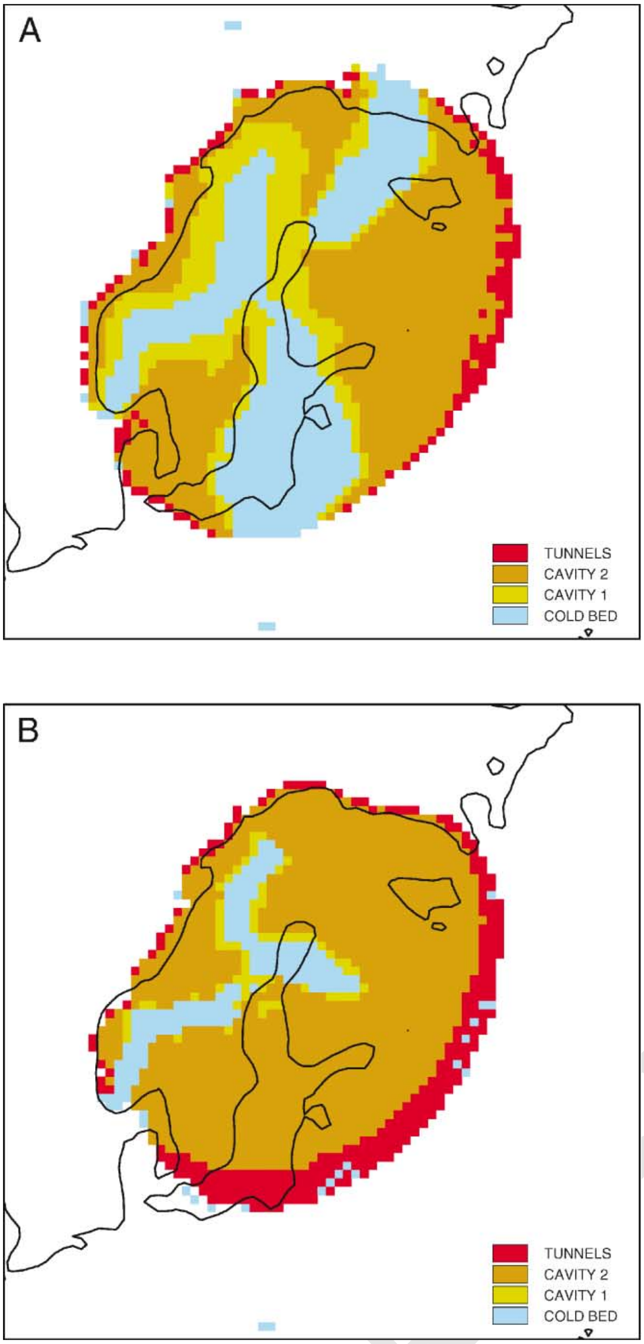

Fig. 5. Ice sheet basal conditions at (a): 18,000 yrs BP; (b): 14,000 yrs BP. Key: cold bed = ice below PMP; cavity 1 = ice at pressure melting point (PMP) but no surface water input, cavity-based drainage; cavity 2 = ice at PMP, surface water input, cavity-based drainage; tunnels = as cavity 2, but tunnel-based drainage.

Throughout the period, almost all of the central area beneath the divide remains frozen, but frozen areas near the margins are more variable, due to the growth and decay of the fast-flowing ice lobes discussed above. This frozen core gets disrupted, but never entirely disappears, during the rapid model deglaciation (Fig. 5b). This is in close agreement with Kleman et al. (1997), who argue that the extensive preservation of landforms older than the LGM in central Scandinavia must imply a frozen bed. They also argue against massive binge-purge cycles (MacAyeal, 1993), affecting large areas of the ice sheet, but favour a stable, frozen core, with an intermediate zone with a 'fractal patchwork' (Kleman et al., 1997, p. 296) of frozen and thawed bed, and an outer wet-bed zone. This again is in qualitative agreement with the model results, which suggest that the development of wet-based, fast flowing lobes during ice sheet growth was spatially and temporally variable. We expect that such a pattern would leave a very complex landscape showing preservation of old features, areas of cross-cutting landforms, and areas typified by complete erosion of previous flow traces occurring in close proximity.

Within the warm based areas of the model ice sheet, basal water drainage is predominantly via linked-cavity systems, although tunnel-based drainage became established around the ice sheet margins during periods of warming climate. This is true during the growth phase, but especially during deglaciation (Fig. 5b), and particularly the final deglaciation after 16,000 yr BP, when increased meltwater fluxes lower sub-glacial water pressures. The warming climate means that large areas of the ice sheet experience surface melt, leading to high water inputs to the basal hydrological system. At this time, tunnels extend up to 160 km from the margin, though lengths of around 80 km are more normal. Typical discharges in sub-glacial tunnels at the ice sheet margin are of the order of 500 $m^3 s^{-1}$ during the early stages of deglaciation (Fig. 6a), when catchment areas are large, falling to around 200 $m^3 s^{-1}$ at 12,000 model years BP (Fig. 6b). These discharges are comparable to the value of 1000 $m^3 s^{-1}$ used by Shreve (1985) for reconstructing ice sheet surface profiles from an esker system in Maine. To obtain such high discharge values, Shreve also assumed that surface melt reached the sub-glacial drainage system.

On account of the long water flow paths and low subglacial hydraulic potential gradients (due to the low ice surface and bed slopes), sub-glacial water pressures are typically 60–80% of ice overburden in tunnel-based systems and 85–95% of ice overburden in linked-cavity systems. Thus, the effect of changes in drainage configuration on ice sheet dynamics is relatively small, as high basal velocities occur even with tunnel-based drainage. This result is obviously dependent on the form of the sliding relationship used, and the parameter values chosen. However, the formation of fast-flowing lobes does not result from switching of the hydrological regime, but from the concentration of water flow into particular areas. This was controlled by the topographic evolution of the ice sheet and was affected only indirectly by the chosen sliding relationship.

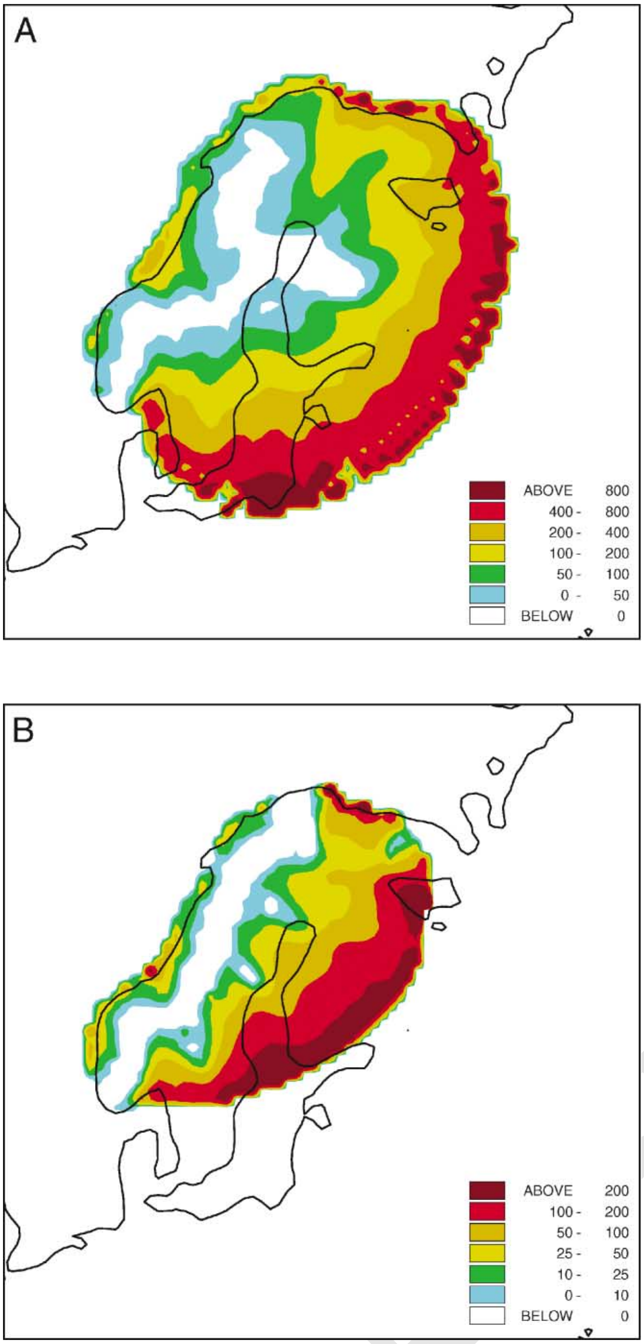

Fig. 6. Subglacial water discharge. (a): At 14,000 yrs BP; (b): At 12,000 yrs BP. Units are $m^3\,s^{-1}$.

5. Model sensitivity to changes in the treatment of ice sheet hydrology

Given the aims of this study, we focus model sensitivity analysis on the hydrological model, rather than on the ice sheet model. There are two main aspects to this; the assumptions and parameter values adopted for the nature of the bed itself, such as tunnel and cavity spacing, bed roughness etc., and the influence of surface-derived meltwater on processes at the bed. This also relates to the thermodynamic scheme adopted here, which does not allow for the advection of cold ice from upstream areas of the ice sheet, and assumes instantaneous transfer of surface temperature changes to the bed. We investigate this by conducting some simple experiments to investigate the control exerted by surface temperature changes on the basal temperature, by lagging the surface temperature changes used as input to the thermodynamic model, to simulate delayed response at the bed.

The earlier, one-dimensional version of the model (Arnold and Sharp, 1992) showed that the main impact of altering the hydrological system parameter values was on the nature of the hydrological system, rather than on the qualitative behaviour of the ice sheet as a whole. Experiments with the two-dimensional model not presented here also showed this. Assuming a smoother bed generally allowed tunnel-based drainage systems to be more common (and vice versa). Through changes in sub-glacial water pressure and hence ice velocity, this altered the exact spatial and temporal distribution of fast flowing lobes, but not their presence or absence. This implies that the development of a lobe at a particular time and place depends on the complex interplay of local ice and bed topography, water availability, and the bed configuration, and would thus be almost impossible to 'predict' in an exact sense.

In this paper we focus more on the role played by the amount of surface water at the bed, through the assumed critical discharge, and the role of basal temperature changes. Altering the degree to which surface melt could reach the bed had a much more profound effect on ice sheet development. Fig. 7 shows time-space diagrams of the extent of fast flow, and its temporal variability, for the period from 30,000 to 10,000 BP, for the NW–SE cross-section through the ice sheet shown in Fig. 1. A range of values of Q_{crit} from 2.5 to 50 $m^3\,s^{-1}$ was used, and a run was also performed in which no surface water is allowed to penetrate to the bed (effectively, an infinite Q_{crit}). This period is chosen as the ice sheet is largest, and so the effects are most apparent. In general, fast flow occurs more frequently as the ice sheet approaches its maximum extent, and during deglaciation. This is broadly climatic, as the warming climate means more meltwater is available. During growth, however, fast flow occurs intermittently, and the nature of the occurrence depends on the value of Q_{crit}. For very low values of Q_{crit} (below c. 5 $m^3\,s^{-1}$) (Fig. 7a), fast flow areas occur on the transect for more of the time, and some episodes last longer than others, although there is little apparent regularity. For Q_{crit} values 5–15 $m^3\,s^{-1}$ (Fig. 7b–e), the episodes of fast flow become more regular in extent and duration; they also tend to last longer, but happen less frequently as Q_{crit} increases. As Q_{crit} increases still further, and when no

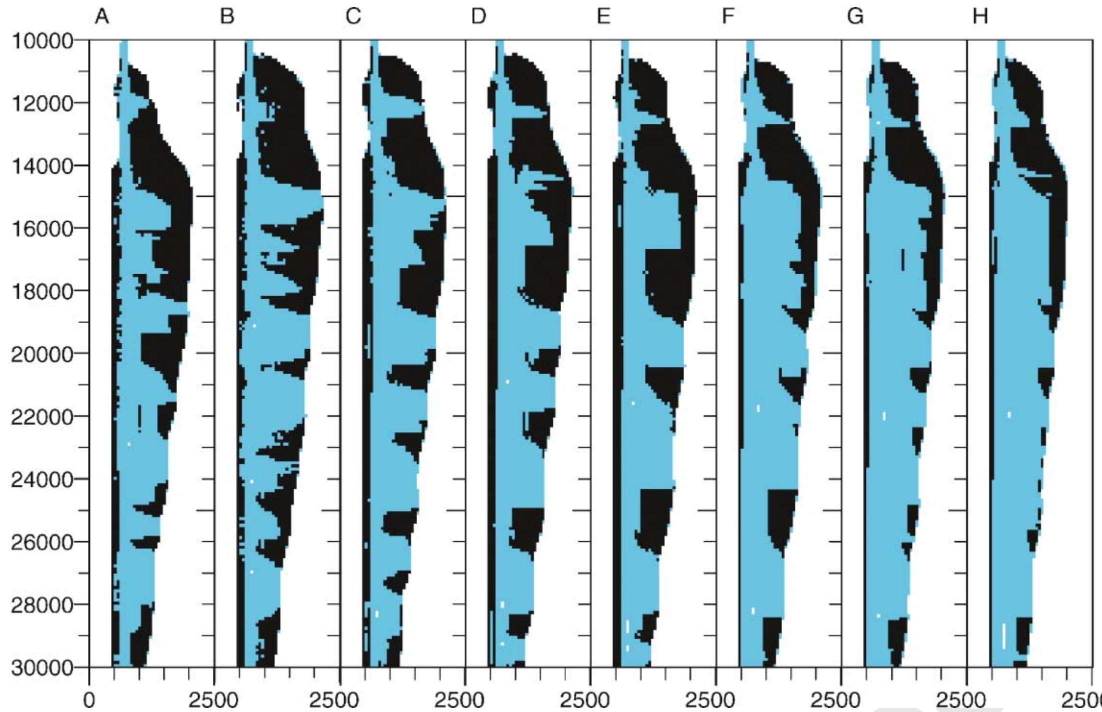

Fig. 7. Time-space diagrams of ice extent, and extent of fast flow from 30,000 yrs BP to 10,000 yrs BP, for transect X–Y in Fig. 1, with variable Q_{crit} values. X-axis units are km; black areas denote fast flow, blue areas denote slow flow. Fast flow is defined as areas of bed at the PMP, and with velocities in excess of $100\,m\,a^{-1}$. $A = Q_{crit}$ of $2.5\,m^3\,s^{-1}$; $B = Q_{crit}$ of $5\,m^3\,s^{-1}$; $C = Q_{crit}$ of $7.5\,m^3\,s^{-1}$; $D = Q_{crit}$ of $10\,m^3\,s^{-1}$; $E = Q_{crit}$ of $15\,m^3\,s^{-1}$; $F = Q_{crit}$ of $20\,m^3\,s^{-1}$; $G = Q_{crit}$ of $50\,m^3\,s^{-1}$; $H =$ infinite Q_{crit} (i.e. no surface water penetration).

surface water can reach the bed (Fig. 7f–h), fast flow becomes much more limited. Only as the ice reaches its maximum extent, and during deglaciation, does it play a significant role.

The spatial pattern of velocity is also affected by the value of Q_{crit}. For lower values a much smoother radial velocity pattern results, with no sharply defined, topographically lower, faster flowing areas (Fig. 8a, for a Q_{crit} of $2.5\,m^3\,s^{-1}$). In these cases, the fast flowing areas seem to cycle on and off across large areas of the ice sheet at once, in a manner analogous to the simple model of 'binge-purge cycles' developed by MacAyeal (1993), although with no obvious periodicity, as discussed above. For Q_{crit} values between around 5 and $15\,m^3\,s^{-1}$, the fast-flowing areas are generally lobate in form, similar to those produced in the 'standard' run. At high Q_{crit} values, the basal hydrology is again much more uniform spatially, with lower water discharges (and consequent lower water pressures in predominantly cavity-based drainage). Spatially patterns of ice flow are more uniform (Fig. 8b, for Q_{crit} of $50\,m^3\,s^{-1}$), driven by the much more uniform pattern of basal melting. This pattern also results if surface melt is not allowed to reach the bed.

Fig. 9 shows time-space diagrams for the runs in which surface temperature changes were lagged for the same time period and transect as Fig. 7. These show some differences between the runs in terms of the exact spatial and temporal pattern of fast flowing areas, but the key qualitative aspects of model behaviour are preserved. No systematic trend in behaviour can be seen, suggesting that basal temperature, whilst affecting the detailed pattern of fast flow, does not play a primary role in controlling its development. The general correspondence in time for the occurrence of fast flow suggests that surface meltwater changes play a larger role than basal temperature changes, although it should be born in mind that the diagram only shows a one-dimensional transect through the ice sheet; fast flow may be occurring in adjacent areas of the ice sheet at times when the transect shown is flowing slowly, due to the spatial variability of fast flow in the model.

6. Discussion

The complex spatial and temporal evolution of the areas of fast flow, particularly during ice sheet growth, demands further explanation. Two aspects of the evolving flow pattern need to be considered: (i) how the lobate nature of the flow becomes established, and (ii) why the extent and location of areas of fast flow varies over time. In addition, this section considers the

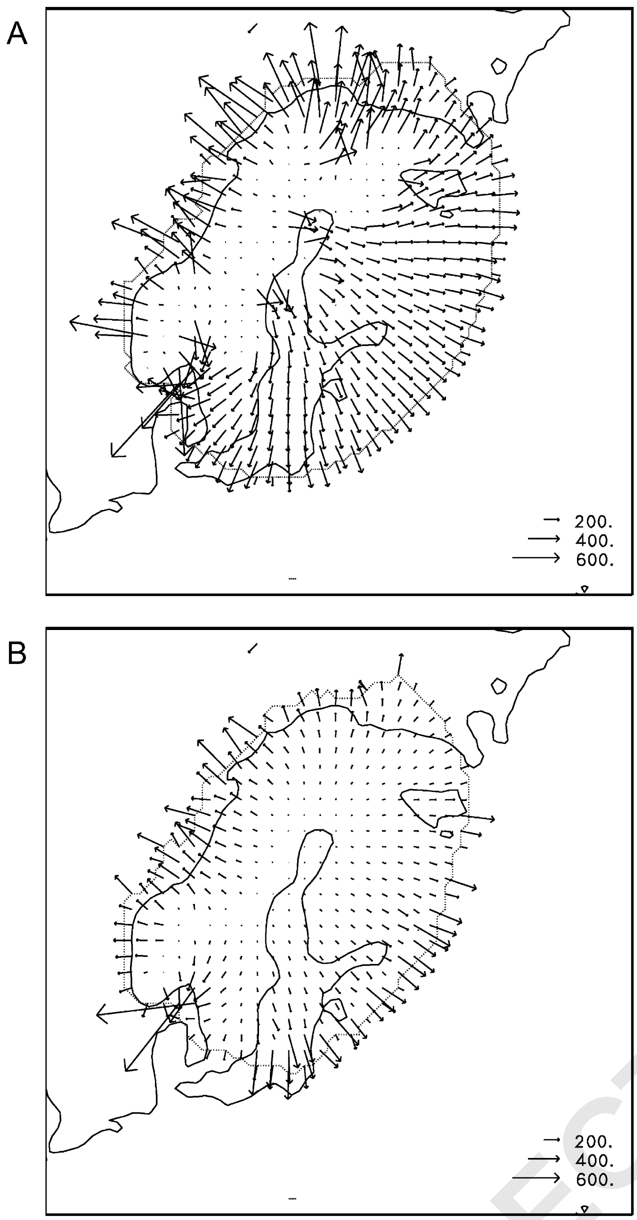

Fig. 8. Ice sheet velocity distributions at 18,000 yrs BP for different values of Q_{crit}. (a): 2.5 $m^3 s^{-1}$; (b): 50 $m^3 s^{-1}$.

impact of fast flow on the overall configuration of the ice sheet.

Due to the combination of high heat production (due to steep surface slopes) and high meltwater availability in marginal areas (within approximately 2–4 grid cells (80–160 km)) of the ice sheet, fast flow initially becomes established in these areas. At the upstream end of areas of fast flow, a 'nick-point' develops in the ice sheet surface. Here, the production of basal heat increases due to the combination of locally steeper surface slope and increasing basal velocity, and this allows head-ward expansion of the areas of fast flow. As this occurs at different rates in different parts of the ice sheet, both surface and basal water flow become concentrated into areas of fast flow, which have the lowest surface elevations. This tends to result in further increases in basal velocity and frictional heating which favour continued head-wards expansion of the fast flowing areas into adjacent areas The lowering of the surface also increases melting, and hence water discharge. This can result in an up-glacier expansion in the area of bed receiving surface melt, a further feedback effect. The spatial concentration of water flow into areas of thinner ice, or topographically lower areas, seems to prevent the whole of the ice sheet margin from experiencing fast ice flow. Flow concentration takes place both at the upstream areas of the lobes and at the lobe margins, where both surface and basal water flow are deflected towards the lobe, rather than towards the ice sheet margin. Bedrock topography plays a role in some areas, especially on the western side of the ice sheet, where topographic variation is strong and topographically controlled fast-flowing areas are relatively constant through time. On the eastern side, where the topography is much flatter, the evolving patterns of ice thickness (which dominate the basal hydraulic potential) are far more important.

The importance for lobe development of this mechanism of water flow concentration by ice sheet topography is underlined by the results of experiments in which the critical discharge value (Q_{crit}) for penetration of surface water to the bed was varied. Allowing surface water to penetrate at smaller discharges (and hence over larger areas) means than flow concentration does not occur. Large areas of the bed begin to receive surface melt, and so flow faster. This thins the ice, ultimately allowing the bed to re-freeze, leading to large-scale 'binge-purge' cycles affecting large areas of the ice sheet. For higher values of Q_{crit}, however, the process of lobe formation discussed above can begin to operate. In this case, individual areas of the ice sheet cycle between fast flow and slow flow, but as a viewed as a whole, the ice sheet is nearly always affected somewhere by fast flow, and so at a larger scale is more stable. As Q_{crit} increases further (or surface water is prevented from penetrating) the potential for flow concentration is reduced, as surface melt only reaches the bed very near the margins. Areas of fast flow are supplied mainly by basal melt, which is much more uniformly distributed spatially.

Several mechanisms combine to restrict the growth of areas of fast flow. As the areas of fast flow expand head-ward, they enter areas of the ice sheet with lower ablation rates. As a result, water flux through the fast flowing areas increases more slowly as these areas grow. This reduces the 'per cell' discharge, especially in upstream areas of the lobes, as the area experiencing fast flow increases more rapidly than water availability. Episodes of climatic cooling also reduce meltwater availability. Both of these effects reduce sliding and

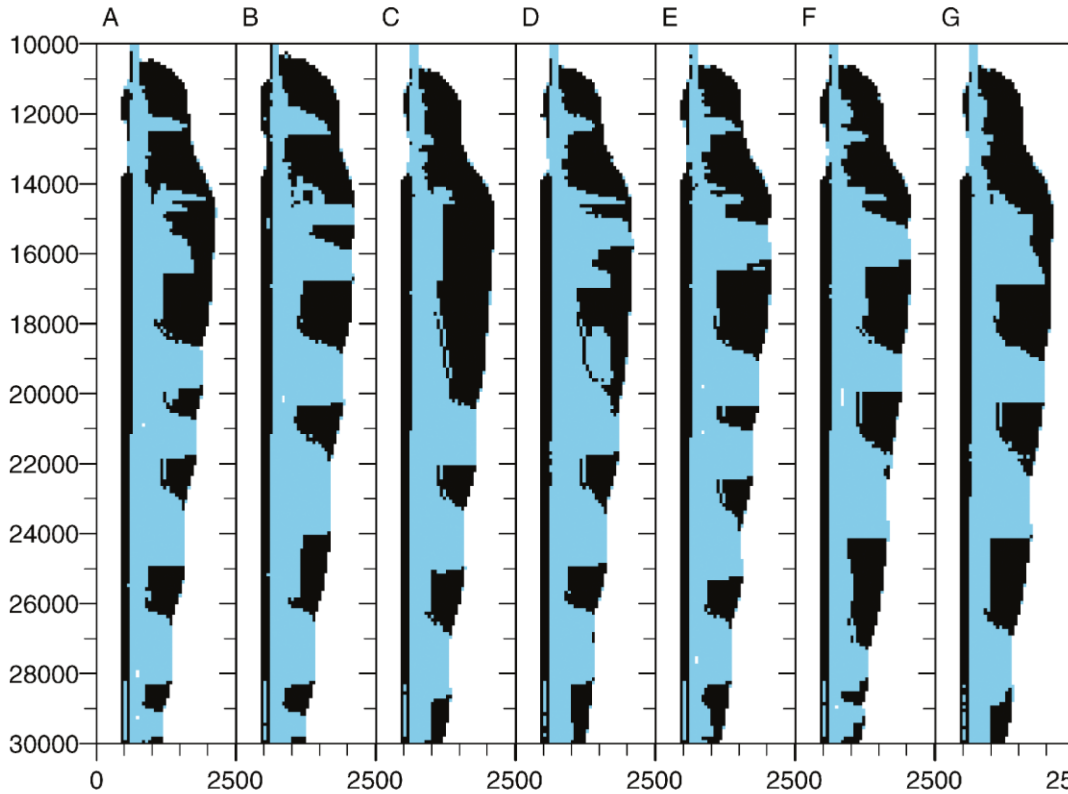

Fig. 9. Time-space diagrams of ice extent, and extent of fast flow from 30,000 yrs BP to 10,000 yrs BP, for transect X–Y in Fig. 1, with lagged surface temperature inputs for basal temperature calculations. X-axis units are km; black areas denote fast flow, blue areas denote slow flow. Fast flow is defined as areas of bed at the PMP, and with velocities in excess of $100\,\mathrm{m\,a^{-1}}$. Lag times: $A = 0$ years (i.e. standard run); $B = 1000$ years; $C = 2000$ years; $D = 5000$ years; $E = 10,000$ years; $F = 15,000$ years; $G = 20,000$ years.

frictional heating (due to the fall in water pressure in cavity-based drainage as water discharge falls), which reduces ice sheet velocity and allows the ice sheet bed to re-freeze. These factors seem to have a much larger, and more immediate impact, than the change in basal temperature due to climate, as shown by the small changes in the qualitative model behaviour where surface temperature changes are lagged at the bed. This perhaps suggests that fracture-induced penetration of surface meltwater to the ice sheet bed is a mechanism by which surface temperature changes might be transmitted very rapidly to the bed. Refreezing of such water at the cold bed would supply latent heat, which together with viscous dissipation, could warm the bed rapidly, allowing sliding and the consequent increase in frictional heating, further aiding the development of fast flow. The basal temperature thus depends very much on changes in local heat production induced by hydrological changes. As velocities fall, surface elevation tends to increase, further reducing ablation rates, concentration of meltwater flow, downstream water flux and the extent of areas of water-lubricated fast sliding. In large lobes, the establishment of tunnel-based drainage near the ice sheet margin results in a small further decrease in water pressure, and hence sliding velocity in such areas. This leads to upstream thickening of the ice, and hence lower water production, which also restricts the headwards growth of the lobes.

Furthermore, as the areas of fast flow expand head-wards into the ice sheet interior, their upper areas start to interact, and 'capture' water from each other. This diversion of water flow rapidly reduces sub-glacial water discharge in the 'captured' lobe. As a result, sliding velocities fall, reducing basal friction and allowing the bed temperature to drop below the melting point. This is illustrated in Fig. 4, which shows how by 18 ka BP the small lobes which existed over Finland (area C) and southern Norway (area A) at 22 ka BP (Fig. 4a) have expanded head-wards into the ice sheet (Fig. 4b), capturing water which previously flowed beneath the 'Baltic Sea' (area B) ice lobe. As a result, this lobe has ceased to exist.

These processes are therefore controlled more by the local variation in basal heat production itself, rather than by the loss of heat to the ice sheet surface. Thus, the rapid switch-off of fast flowing areas would seem quite realistic; the reduction in heat production due to the thinner ice and lower ice velocity as water pressures drop would be felt very rapidly at the bed, independently of the rate of heat loss due to thinning ice and/or surface temperature changes being conducted to the bed. This again would seem to be born out by the insensitivity of the model to 'lagged' surface temperature changes.

A fundamental problem therefore seems to be what mechanisms control the oscillation of the bed about the pressure melting point. The two possible controls would seem to be the climate changes at the surface, or the changes in ice sheet geometry and dynamics, and the resulting changes in basal heat production. The fact that lagging surface temperature changes at the bed makes little overall difference to the model results seems to suggest that the latter mechanism dominates, and that the impact of surface temperature changes on basal temperature is less important. However, the fact that fast flow does tend to occur at certain times more frequently than at others, and also occurs over a wider area of the ice sheet during warming episodes (especially the main deglaciation phase after ~18,000 BP) suggests that surface temperature changes can be important. Thus, some mechanism to allow the (near) instantaneous transfer of surface temperature changes to the bed must also be required; the penetration of surface meltwater to the bed, possibly by fracture propagation, would seem to provide this. The role of surface temperature variations on changing in basal temperature would seem to be further complicated by the fact that during the last 20,000–30,000 years of a glacial cycle, a series of temperature perturbations driven by Dansgaard–Oerscher events will be arriving at the bed. This may well affect the precise timing of basal warming and cooling in particular areas, but it would not seem to invalidate the major controls on basal conditions explored in this study, and their impact on ice sheet dynamics.

As discussed above, these changes in ice sheet hydrology and velocity seem to match qualitatively with geological reconstructions of the dynamics of the Scandinavian ice sheet. These have shown lobate patterns of flow in the central areas of Scandinavia, and also rather complex evolution of these patterns spatially and temporally (e.g. Kurimo, 1978; Punkari, 1984; Kleman et al., 1997). The predicted mode of retreat of the ice sheet, in which an area of tunnel-based sub-glacial drainage near the ice sheet margin retreats up-glacier as the margin retreats, also matches well with geological evidence for esker formation and glacier dynamics in southern Sweden. This suggests that eskers were formed time-transgressively beneath a retreating ice sheet margin (Hebrand and Åmark, 1989).

The relatively thin model ice sheet has a more linear surface profile on its eastern margin than in the west. This contrasts with the ice sheet morphology produced by models without basal slip, which show a parabolic profile with rapid thickening away from the margin. The linear surface profile is largely caused by the high ice discharge from central areas into the ice lobes. The new reconstruction matches well with isostatically based reconstructions of the Scandinavian ice sheet (Lambeck et al., 1998). These suggest that, for plausible values of lithosphere thickness and mantle viscosity, maximum ice sheet thicknesses at the LGM are around 2000 m, located to the west of the Gulf of Bothnia, compared with the 3400 m thick ice sheet divide over the Gulf of Bothnia suggested by Denton and Hughes (1981). The thinner, isostatically derived ice sheet thicknesses are similar to those produced in the model discussed here, which suggests thicknesses of around 1800 m over the Gulf of Bothnia, and 2000 m at the divide, slightly to the west.

The results of this study, in which the ice sheet as a whole is affected by fast flow in some areas throughout growth and decay of the ice sheet, but particularly during deglaciation, also agree qualitatively with the reconstructions of Boulton et al. (2001). They argue that perennial streaming would be a mechanism to reconcile the apparent mismatch in ice thickness between most model-based reconstructions, and the isostatic evidence for ice thickness discussed above.

7. Conclusions

Inclusion of basal hydrology in a model of the Scandinavian Ice Sheet produces behaviour that seems to match qualitatively with that inferred from geological evidence. Spatially and temporally variable zones of fast flow develop within the ice sheet through mechanisms which are entirely internal to the model, and are not contingent upon the specification of locally distinct basal boundary conditions for their formation (c.f. Holmlund and Fastook, 1993). The presence of extensive areas of fast flow results in a relatively thinner ice sheet, particularly in central and eastern Scandinavia. This matches well with isostatically based reconstructions of ice sheet thickness. The variability of the warm-bedded fast-flowing areas in the standard run, located towards the margin from a frozen-bed 'core' area within the ice sheet also matches well with geological evidence, and seems to argue against massive binge-purge cycles affecting large areas of an ice sheet (Macayeal, 1993); rather, the flow variability is manifest at a more local scale within the ice sheet.

The mechanism by which fast flow occurs in the model involves the accentuation of the impact of initial changes in basal temperature by the concentration of meltwater flow into those areas where the basal ice reaches the pressure melting point. Flow concentration is linked to changes in ice sheet surface topography and their effect on the form of the sub-glacial hydraulic potential surface. The model also shows that discrete areas of fast flow develop when surface melt is input to the bed of the ice sheet in particular areas. They do not develop when surface water inputs are absent or distributed across the entire ice sheet ablation area.

Concentration of meltwater flow, both on the surface of the ice sheet and at the bed (due to variations in the sub-glacial hydraulic potential), tends to increase sub-glacial water pressures (due to the distributed nature of the drainage system over much of the bed). Through the water-pressure dependent sliding law, this increases basal sliding and heat production. In turn, this causes further changes in ice sheet geometry and patterns of surface and basal water flow and results in headwards growth of areas of fast flow. This positive feedback cycle is halted by a series of factors that eventually limit the availability of water at the base of the ice sheet. The formation of discrete areas of fast flowing ice, separated by slower ice, has been observed in other ice sheet models. It is due to interactions between ice flow, basal temperature and basal sliding (e.g. Payne and Dongelmans, 1997; Payne et al., 2000), or to interactions between ice temperature and rates of ice deformation (e.g. Payne and Baldwin, 1999). Thus, the spatial differentiation of flow produced in this study is not unique. What seems to be new to this model, however, is the temporal variability of flow within the lobes. This has been observed in a two-dimensional flowline ice sheet model (e.g. Payne, 1995). However, it does not generally occur in map-plane models (either two-dimensional or three-dimensional), in which the ice lobes seem to be more permanent features (e.g. Payne and Dongelmans, 1997; Payne and Baldwin, 1999; Payne et al., 2000). The exception to this is the study by Payne (1998), in which the Siple Coast area of West Antarctica does show temporal flow variability, as fast flowing areas seem to 'capture' ice from each other. In the current study, however, the variations in hydrology driven by the impact of topographic changes acting internally to the model allow fast flowing areas to switch on and off. This is due to processes occurring within the lobes themselves, as well as to interactions between the lobes through a *water* capture mechanism. Climatic changes can also lead to hydrological changes (due to varying water discharges, and hence water pressure) and can act as an external forcing mechanism, increasing flow variability.

The model does not include the effect of advection of cold ice from upstream (or laterally from inter-lobate areas). If included in the model, this might also slow the head-ward penetration of the zones of fast flow into the ice sheet interior. However, it is unlikely that this would preclude the basic mechanism by which changes in ice sheet topography lead to concentration of water flow into particular areas of the ice sheet. Neither would it preclude the possibility that these areas interact to cause switches in the flow regime in other parts of the ice sheet. Nevertheless, work is underway to include the physically based treatment of basal hydrology developed here in a full thermo-mechanically coupled ice sheet model to address this issue.

Acknowledgements

This work was undertaken while NA held a UK Natural Environment Research Council Studentship at Cambridge University, and the manuscript was begun while NA held an Isaak Walton Killam Memorial Post-doctoral Fellowship at the University of British Columbia. We also thank the referees, Richard Hindmarsh, Neil Humphrey, Garry Clarke and Tony Payne for their helpful comments on the manuscript.

Appendix A. Model formulation

The ice dynamics model used here is a conventional, two-dimensional planar model for ice flow. All parameter values are given in Table 1. It uses the continuity equation to calculate the evolution of ice thickness through time

$$\frac{\partial Z}{\partial t} = \mathrm{Ac} - \mathrm{Ab} - \nabla(\bar{U}Z), \tag{A.1}$$

where Z is the ice thickness, ∇ the two-dimensional horizontal divergence operator, A_c the local accumulation rate, A_b the local ablation rate and $\bar{U}$ the vertically integrated two-dimensional horizontal velocity, resulting from deformation of the ice, and in certain circunstances, sliding of the ice over its bed. This is solved using a semi-implicit, alternating direction implicit finite difference scheme, following Press et al. (1992).

Ice deformation is assumed to be driven solely by the horizontal basal shear stresses (τ_b), which are approximated by

$$\tau_{bx} = \rho_i g Z \frac{\partial E}{\partial x} \tag{A.2}$$

in the x direction, where E is the ice surface elevation, g is gravity, and ρ_i is ice density, and similar for the y direction.

The resulting vertically integrated ice deformation velocity is then calculated from Glen's flow law

$$U_{dx} = \frac{2A}{n+2}\tau_b^{n-1}\tau_{bx}Z, \tag{A.3}$$

where U_{dx} is the x component of the deformation velocity, A is the temperature dependent Arrhenius relation, and n is usually taken to be 3. τ_b is derived from the two-dimensional surface slope, in an equivalent equation to A2. This relationship assumes that ice deformation is laminar, and occurs under simple shear, and is unaffected by longitudinal stresses.

Table 1
Model parameter values

Ice flow			
Deformation			
Multiplier	A	5.3×10^{-15}	$\mathrm{s^{-1}\,k\,Pa^{-3}}$
Power	n	3.0	—
Sliding			
1st multiplier	K_1	6.3×10^{-5}	$\mathrm{m^2\,s^{-1}\,k\,Pa^{-1}}$
2nd multiplier	K_2	400	M
Drainage configuration			
Latent heat	L	3.3×105	$\mathrm{J\,kg^{-1}}$
Channel flow	f	700	$\mathrm{m^{-8/3}\,kg}$
No. of cavities	N_K	30000	—
Cavity X-section	S_K	10^{-2}	$\mathrm{m^2}$
Shadowing function	S	0.5	—
Bedrock amplitude	a	1	m
Bedrock wavelength	l	5	m
Ratio a/l	v	0.2	—
Power function	m	2.0	—
Ice conductivity	K	2.1	$\mathrm{J\,s^{-1}\,m^{-1}\,K^{-1}}$
Ice density	ρ_i	900	$\mathrm{kg\,m^{-3}}$
Water density	ρ_w	1025	$\mathrm{kg\,m^{-3}}$
Gravity	G	9.81	$\mathrm{m\,s^{-2}}$
Isostasy			
Mantle density	ρ_m	3300	$\mathrm{kg\,m^{-3}}$
Mantle diffusivity	Da	1.11	$\mathrm{m^2\,s^{-1}}$
Precipitation parameterisation			
	c_1	0.8	$\mathrm{m\,a^{-1}}$
	c_2	0.004	$\mathrm{m\,a^{-1}}\Psi^{-}$
	c_3	0.003	$\mathrm{m\,a^{-1}}\varphi^{-}$
	c_4	25000	—
	c_5	2500	m
	c_6	10	$\mathrm{m}\Psi^{-1}$
	c_7	25	$\mathrm{m}\varphi^{-}$
	c_8	0.85	—
	c_9	1000	—

Sliding velocity also depends to some extent on the local basal shear stress, but is also assumed to be water pressure dependent. We use the sliding 'law' of McInnes and Budd (1984)

$$U_{\mathrm{S}X} = k_1 \tau_{\mathrm{b}X}/(N + k_2 N^2), \tag{A.4}$$

where $U_{\mathrm{s}x}$ is the x component of the sliding velocity, N is the calculated effective pressure (that is, the ice overburden pressure minus the subglacial water pressure), and k_1 and k_2 are empirical parameters.

Sliding only occurs if the bed is at the pressure melting point, and we use a simple scheme to calculate the basal temperature, based on the heat supplied to the bed by geothermal heating and friction from ice movement, and the temperature gradient needed to conduct that heat away. The frictional heat supplied to the bed (H) is calculated from

$$H = \rho_\mathrm{i} \frac{\mathrm{d}E}{\mathrm{d}x} Q_\mathrm{i}, \tag{A.5}$$

where Q_i is the ice discharge. It can be assumed that this heating occurs only at the bed, and so this, together with the geothermal heat flux (G) can then be compared with the temperature gradient needed to conduct the heat away

$$H + G = K \frac{\partial T}{\partial z}, \tag{A.6}$$

where $\partial T/\partial z$ is the vertical temperature gradient and K the thermal conductivity of ice. If the surface temperature is known, the basal temperature can be calculated from

$$T_\mathrm{b} = T_\mathrm{s} + ZH/K, \tag{A.7}$$

where T_b is the basal temperature, and T_s the surface temperature. Any excess heat is used to melt basal ice. T_s is calculated from the climatic forcing, the ice sheet elevation, and the equilibrium line altitude, assuming a temperature at the equilibrium line of $-15^\circ\mathrm{C}$ (Oerlemans, 1982).

The model calculates the effective pressure using the equations of Fowler (1987a). The effective pressure varies depending on whether the basal drainage system consists of large, widely spaced, efficient conduits or tunnels, or an inefficient system of linked cavities.

For tunnels, effective pressure is calculated as

$$N_R = [(\rho_\mathrm{w} g \phi Q_R)/(\rho_\mathrm{i} A F S_K)]^{1/n}, \tag{A.8}$$

where N_R is the effective pressure for a tunnel based system, ρ_w the water density, g the acceleration due to gravity, Q_R the volume flux of meltwater, ρ_i the ice density, A the Arrhenius parameter, F the latent heat, n the exponent in Glen's flow law, S_R the tunnel cross sectional area, and ϕ is the hydraulic gradient, defined as

$$\phi = \alpha + [(\rho_\mathrm{w} - \rho_\mathrm{i})/\rho_\mathrm{w}]\beta. \tag{A.9}$$

Here β is the bed slope. S_R is calculated as

$$S_R = (f Q_R^2/\rho_\mathrm{w} g \phi)^{3/8}, \tag{A.10}$$

where f is an empirical constant related to turbulent channel flow.

For cavities, effective pressure is calculated as

$$N_K = r[(\rho_\mathrm{w} g \phi)/(\rho_\mathrm{i} A F)(Q_K n_K S_K)]^{1/n}, \tag{A.11}$$

where N_K is effective pressure for a cavity based system, r is a shadowing function (Lliboutry, 1978), defined as the probability that a randomly selected area of the bed is in contact with the ice, $Q_K = Q_R$ the volume flux of meltwater, n_K is the number of passageways across the width of the glacier and S_K is the cross-sectional area of a typical passageway.

Following Fowler (1987a), a stability criterion for tunnel flow is used to determine which type of system exists in each grid cell at each time-step

$$\Lambda = vU_s/1AN^n \tag{A.12}$$

where $v = (a/l)$, a is typical bedrock bump amplitude, l is typical bump wavelength and A is the Arrhenius parameter.

The critical value for tunnel stability, Λ_c, is given by

$$\Lambda_c = (3nS_R/A^*)^{[(4-\mu)/\mu]} \tag{A.13}$$

where A^* is the total cavity cross sectional area, and μ the power function for self-similar bedrocks (Fowler, 1987a, b).

This criterion assumes that a tunnel-based system can exist alongside a cavity-based system, which will drain areas of the bed between the tunnels. The stability criterion calculates the stability of the tunnel-based system in the presence of cavities, by comparing the relative changes in water pressure as discharge changes in the two systems. Tunnel-based systems are generally stable for situations with high water discharge, low water pressure and slow-moving ice. If tunnels are found to be stable, they are assumed to dominate the drainage system and to carry all of the sub-glacial water. Water pressure is calculated accordingly (Eq. (A.8)). If tunnels are unstable, the water is assumed to drain through a cavity-based system, and Eq. (A.11) for cavity-based drainage is used. Fowler's published values for the bed roughness parameters and cavity size and spacing are used throughout the model (Table 1). If tunnel-based drainage is predicted, it is assumed that there is one tunnel in each 40 km grid cell, consistent with the observed esker spacing of approximately 30 kmin southern Finland (Geological Survey of Finland, 1984).

Eqs. (A.6) and (A.9) both require the subglacial discharge to be known. To calculate this, surface melt is routed across the ice sheet surface using an 'upstream contributing area' algorithm described by Sharp et al. (1993). Water discharge is integrated along each flow path until it exceeds the critical value, at which point it is added to the rate of basal melt in that cell. The same 'upstream contributing area' algorithm is used to calculate basal discharge in each cell by integrating the combined surface and basal inputs down the sub-glacial hydraulic potential surface

$$\Phi = \rho_w gB + \rho_i gZ, \tag{A.14}$$

(Shreve, 1972) where B is the bedrock elevation, until the ice sheet margin is reached. This method assumes that meltwater generated in interior regions of an ice sheet can reach the margin in less than one model time step For a 1500 km wide ice sheet and 10 year time step, this implies that water flows at $> 5 \times 10^{-3}\,\mathrm{m\,s^{-1}}$. Dye tracing results from modern glaciers generally yield flow velocities higher than this (e.g. Behrens et al., 1975; Fountain, 1993), although it is of similar magnitude to velocities in distributed systems.

The model makes separate calculations of accumulation and ablation rates over the ice sheet. Precipitation rates across the study area at 120 ka BP were assumed to be the same as at the present day. This distribution was modelled using empirical relationships, which relate precipitation to latitude, longitude and elevation. During the model run, precipitation rates were altered as a function of the imposed temperature forcing and additional cooling associated with elevation changes induced by ice sheet growth and decay. These relationships to do not account for possible changes of the atmospheric circulation that may have resulted from ice sheet growth and decay. They assume that a 'sea-level equivalent' precipitation (P_0) value can be defined for north-west Europe, based largely on distance from the Atlantic Ocean (assumed to be the main water vapour source), latitude, and temperature. This precipitation value thus decreases towards the north and east

$$P_0 = c_1 - c_2\psi - c_3\varphi - c_4\Delta E_0, \tag{A.15}$$

where ψ is the longitude, φ the latitude, ΔE_0 the change in elevation of the $1\,\mathrm{m\,a^{-1}}$ ablation contour (see below), and c_1 to c_4 are adjustable parameters.

This calculated 'sea level' precipitation is then subjected to orographic enhancement, up to a critical height (E_m), at which moisture exhaustion is assumed to occur, and above which precipitation will start to decrease. This critical height again depends on latitude, longitude and temperature change

$$E_m = c_5 - c_6\psi - c_7\varphi - c_8\Delta E_0, \tag{A.16}$$

where c_5 to c_8 are again adjustable parameters. The precipitation value (P_m) at this altitude is then calculated from

$$P_m = P_0(2^{E_m/c_9}), \tag{A.17}$$

where c_9 is an adjustable parameter. From P_0, P_m and E_m, a precipitation gradient with altitude is calculated (P_g), and the actual precipitation value (P) in a particular grid cell, at a particular surface elevation (E) is calculated from

$$P = [P_0 + EP_g] - P_m(2^{(E-E_m)/c_9}) + [P_0 + EP_g] \tag{A.18}$$

if $E < E_m$, and

$$P = P_m/(2^{(E-E_m)/c_9}) \tag{A.19}$$

if $E \geqslant E_m$.

Values for c_1 to c_9 were derived by making an initial guess for their values, and then approximating optimal values by comparing the resulting predicted precipitation field by eye for western Europe with published precipitation maps (UNESCO, 1970). Accumulation rates (A_c) were calculated from predicted precipitation values using an empirical effectiveness relationship

(Payne, 1988)

$$\mathrm{Ac} = -0.698P + 0.014\varphi + 0.224\Delta E_0. \tag{A.20}$$

Values of c_4 and c_8, which control the response to climate change were adjusted by running the model with different values until predicted ice sheet extent approximately matched that inferred from geological evidence.

Ablation rates were calculated using the method of Budd and Smith (1981).

$$\log_{10} \mathrm{Ab} = \tfrac{1}{\kappa}(E_0 - E), \tag{A.21}$$

where E_0 is the elevation of the $1\,\mathrm{m\,a^{-1}}$ ablation contour, which is itself a function of latitude and the imposed temperature change, converted to an elevation change using a standard lapse rate of $6.5^\circ\mathrm{C\,km^{-1}}$.

Calving rates at marine margins of the ice sheet were determined using a water depth dependent calving law (Brown et al., 1982)

$$V_\mathrm{c} = 27.1W, \tag{A.22}$$

where V_c is a calving velocity, and W is the water depth at the ice margin. V_c is converted to a volume loss by multiplying by the ice thickness in a calving cell. This is incoprorated into the continuity equation by adding any calving to the ablation rate. These relationships all have obvious limitations. However, there are still enormous uncertainties about the climate during the last glacial period. We therefore justify the use of these relationships on the grounds that our aim is to investigate how the dynamics of the model ice sheet are affected by the inclusion of a physically based model of sub-glacial hydrology. We emphasise that we have not tried to produce as 'geologically realistic' a simulation of the ice sheet as possible.

Isostatic response is calculated using a diffusion-based scheme

$$\frac{\partial B}{\partial t} = \mathrm{Da}\nabla^2(B - B_\mathrm{o} + L), \tag{A.23}$$

where Da is mantle diffusivity, B_o is the original unloaded topography, and L is the imposed load, defined as $Z\rho_\mathrm{i}/\rho_\mathrm{m}$, where ρ_m is the mantle density.

References

Allen, J.R.L., 1971. A theoretical and experimental study of climbing-ripple cross-lamination, with a field application to the Uppsala esker. Geografiska Annaler 53A, 157–187.

Alley, R.B., 1989. Water pressure coupling of sliding and bed deformation: I. Water system. Journal of Glaciology 35, 108–118.

Arnold, N., Sharp, M., 1992. Influence of glacier hydrology on the dynamics of a large quaternary ice sheet. Journal of Quaternary Science 7, 109–124.

Banerjee, I., McDonald, B.C., 1975. Nature of esker sedimentation. In: Jopling, A.V., McDonald, B.C. (Eds.), Glaciofluvial and glaciolacustrine sedimentation. Society of Economic Palaeontologists and Mineralogists, Special Publication 23, Tulsa, OK, pp. 132–154.

Behrens, H., Bergmann, H., Moser, H., Ambach, W., Jochum, O., 1975. On the water channels of the Hintereisferner, Ötztal Alps, Austria. Journal of Glaciology 14, 375–382.

Bentley, C.R., 1987. Antarctic ice streams: a review. Journal of Geophysical Research 92 (B9), 8843–8858.

Blatter, H., 1987. On the thermal regime of an Arctic valley glacier—a study of White Glacier, Axel-Heiberg island, NWT, Canada. Journal of Glaciology 33, 200–211.

Bond, G., Heinrich, H., Broeker, W., Labeyrie, L., McManus, J., Andrews, J., Huon, S., Jantschik, R., Clasen, S., Simet, S., Tedesco, K., Bonani, G., Ivy, S., 1992. Evidence for massive discharges of icebergs into the North Atlantic during the last glacial period. Nature 360, 245–249.

Boulton, G.S., Caban, P., 1995. Groundwater flow beneath ice sheets: Part II—its impact on glacier tectonic structures and moraine formation. Quaternary Science Reviews 14, 563–587.

Boulton, G.S., Caban, P., 1995a. Groundwater flow beneath ice sheets: Part I—Large scale patterns. Quaternary Science Reviews 14, 545–562.

Boulton, G.S., Clark, C.D., 1990b. A highly mobile Laurentide ice sheet revealed by satellite images of glacial lineations. Nature 346, 813–817.

Boulton, G.S., Clark, C.D., 1990. The Laurentide ice sheet through the last glacial cycle: the topology of drift lineations as a key to the synamic behaviour of former ice sheets. Transactions of the Royal Society of Edinburgh, Series Earth Science 81, 327–347.

Boulton, G.S., Dongelmans, P., Punkari, M., Broadgate, M., 2001. Palaeoglaciology of an ice sheet through a glacial cycle: the European ice sheet through the Weichselian. Quaternary Science Reviews 20, 591–625.

Boulton, G.S., Hindmarsh, R.C.A., 1987. Sediment deformation beneath glaciers: rheology and geological consequences. Journal of Geophysical Research 92 (B9), 9059–9082.

Brown, C.S., Meier, M.F., Post, A., 1982. Calving speed of Alaska tidewater glaciers, with application to Columbia Glacier. US Geological Survey Professional Paper 1258-C., 15pp.

Budd, W.F., Smith, I.N., 1981. The growth and retreat of ice sheets in response to orbital radiation changes. Sea level, Ice and Climatic Change. Proceedings of the Canberra Symposium, December 1979. IAHS Publication no. 131, 369–409.

Clark, C.D., 1993. Mega-scale glacial lineations and cross-cutting ice-flow landforms. Earth Surface Processes and Landforms 18, 1–29.

Clark, P.U., Walder, J.S., 1992. Subglacial drainage and deforming beds beneath the Laurentide, British and Scandinavian ice sheets. EOS, Transactions of the American Geophysical Union 73, 159–160 (Abstract only).

Dansgaard, W., Johnsen, S.J., Clausen, H.B., Gundesrup, N., 1973. Stable isotope glaciology. Meddelelser om Grønland 197, 53.

Dansgaard, W., Johnsen, S.J., Clausen, H.B., Dahl-Jensen, D., Gundestrup, N.S., Hammer, C.U., Hvidberg, C.S., Steffensen, J.P., Sveinbjörnsdottir, A.E., Jouzel, J., Bond, G., 1993. Evidence for general instability of past climate from a 250-kyr ice-core record. Nature 364, 218–220.

Denton, G.H., Hughes, T.J., 1981. The Last Great Ice Sheets. Wiley, New York, 484pp.

Dyke, A.S., Morris, T.F., 1988. Canadian landform examples 7. Drumlin fields, dispersal trains and ice streams in arctic Canada. The Canadian Geographer 32, 86–90.

Dyke, A.S., Prest, V.K., 1987. Last Wisconsinan and Holocene history of the Laurentide ice sheet. Geographie et Physique Quatenaire 41, 237–264.

Engelhardt, H., Kamb, B., 1997. Basal hydraulic system of a West Antarctic ice stream: constraints from borehole observations. Journal of Glaciology 44, 223–230.

Engelhardt, H., Kamb, B., 1998. Basal sliding of Ice Stream B, West Antarctica. Journal of Glaciology 44, 223–230.

Fountain, A.G., 1993. Geometry and flow conditions of subglacial water at South cascade glacier, Washington state, USA; an analysis of tracer injections. Journal of Glaciology 30, 180–187.
Fowler, A.C., 1987a. Sliding with cavity formation. Journal of Glaciology 33, 255–267.
Fowler, A.C., 1987b. A theory of glacier surges. Journal of Geophysical Research 92 (B9), 9111–9120.
Fowler, A.C., Johnson, C., 1995. Hydraulic runaway: a mechanism for thermally regulated surges of ice sheets. Journal of Glaciology 41, 554–561.
Fowler, A.C., Johnson, C., 1996. Ice sheet surging and ice-stream formation. Annals of Glaciology 23, 68–73.
Fowler, A.C., Schiavi, E., 1998. A theory of ice sheet surges. Journal of Glaciology 44, 104–118.
Geological Survey of Finland, 1984. Quaternary Deposits of Finland. 1 : 1,000,000.
Hebrand, M., Åmark, M., 1989. Esker formation and glacier dynamics in eastern skåne and adjacent areas, southern Sweden. Boreas 18, 67–81.
Holmlund, P., Fastook, J., 1993. Numerical modelling provides evidence of a Baltic Ice Stream during the Younger Dryas. Boreas 22, 77–86.
Huybrechts, P., 1992. The Antarctic ice sheet and environmental change: a three-dimensional modelling study. Berichte zur Polarforschung 99, 241.
Iken, A., 1974. Velocity fluctuations of an Arctic valley glacier, a study of White Glacier, Axel Heiberg Island, Canadian arctic Archipelago. Axel Heiberg Island Research Reports, McGill University, Montreal, Canada, Glaciology No. 5, 116pp.
Iken, A., 1981. The effect of the subglacial water pressure on the sliding velocity in an idealised numerical model. Journal of Glaciology 27, 407.
Iverson, N.R., Jansson, P., Hooke, R.L., 1995. Flow mechanism of glaciers on soft beds. Science 267, 80–81.
Johnsen, S.J., Clausen, H.B., Dansgaard, W., Fuhrer, K., Gundestrup, N., Hammer, C.U., Iversen, P., Jouzel, J., Stauffer, B., Steffensen, J.P., 1992. Irregular glacial interstadials recorded in a new Greenland ice core. Nature 359, 311–313.
Kamb, B., 1987. Glacier surge mechanism based on linked cavity configuration of the basal water conduit system. Journal of Geophysical Research 92 (B9), 9083–9100.
Kleman, J., Hättestrand, C., Borgström, I., Stroeven, A., 1997. Fennoscandian palaeoglaciology reconstructed using a glacial geological inversion model. Journal of Glaciology 43, 283–299.
Kurimo, H., 1978. Late-glacial ice flows in northern Kainuu and Peräpohjola, north-east Finland. Fennia 156, 11–43.
Lambeck, K., Smither, S., Johnston, P., 1998. Sea-level change, glacial rebound and mantle viscosity for Northern Europe. Geophysical Journal International 134, 102–144.
Le Meur, E., Huybrechts, P., 1996. A comparison of different ways of dealing with isostasy: examples of modelling the Antarctic ice sheet during the last glacial cycle. Annals of Glaciology 23, 309–317.
Lindstrom, D.R., 1990. The eurasian ice sheet formation and collapse resulting from natural atmospheric CO_2 concentration variation. Paleoceanography 5, 207–227.
MacAyeal, D.R., 1993. Binge/purge oscillations of the Laurentide ice sheet as a cause of the North Atlantic's Heinrich events. Paleoceanography 8, 775–784.
Mathews, W.H., 1974. Surface profiles of the Laurentide Ice Sheet in its marginal areas. Journal of Glaciology 13, 37–43.
Mavlyudov, B.R., 1995. Problems of en- and subglacial drainage. Annales littéraires de l'université de Besancon, no. 561, série Géographie no. 34. Actes du troisieme symposium international Cavités glaciaires et cryokarst en régions polaires et de haute montagne. Chamonix, France, September 1994, pp. 77–82.
Mavlyudov, B.R., 1998. Glacier caves origin. Salzburger Geographische Materialien. Vol. 28. Fourth international symposium on glacier caves and cryokarst in polar and high mountain regions, September 1996. Salzburg, Austria, pp. 123–130.
McInnes, B.J., Budd, W.F., 1984. A cross-sectional model for West Antarctica. Annals of Glaciology 5, 95–99.
Paterson, W.S.B., 1994. The Physics of Glaciers, 3rd Edition. Pergamon/Elsevier, Oxford.
Payne, A.J., 1988. Modelling former ice sheets. Ph. D. Thesis, Edinburgh University, Edinburgh, UK, 211pp.
Payne, A.J., 1995. Limit cycles in the basal thermal regime of ice sheets. Journal of Geophysical Research 100 (B3), 4249–4263.
Payne, A.J., 1998. Dynamics of the Siple Coast ice streams, West Antarctica: results from a thermomechanical ice sheet model. Geophysical Research Letters 25, 3173–3176.
Payne, A.J., 1999. A thermomechanical model of ice flow in West Antarctica. Climate Dynamics 15, 115–125.
Payne, A.J., Dongelmans, P.W., 1997. Self-organisation in the thermomechanical flow of ice sheets. Journal of Geophysical Research 102 (B6), 12219–12233.
Payne, A.J., Huybrechts, P., Abe-Ouchi, A., Calov, R., Fastook, J.L., Greve, R., Marshall, S.J., Marsiat, I., Ritz, C., Tarasov, L., Thomassen, M.P.A., 2000. Results from the EISMINT model intercomparison: the effects of thermomechanical coupling. Journal of Glaciology 46, 227–239.
Punkari, M., 1984. The relations between glacial dynamics and tills in the eastern part of the Baltic Shield. In: Konigsson, L.-K. (Ed.), Ten Years of Nordic Till Research, Vol. 20. Striae, pp. 49–54.
Punkari, M., 1989. Glacial dynamics and related erosion-deposition processes in the Scandinavian ice sheet in south-western Finland: a remote sensing, fieldwork and computer modelling study. Helsinki, Academy of Finland. Research Council for the Natural Sciences. Final Report, Project 01/663. 86pp.
Röthlisberger, H., 1972. Water pressure in intra- and subglacial channels. Journal of Glaciology 11, 177–203.
Scambos, T.A., Hulbe, C., Fahnestock, M., Bohlander, J., 2000. The link between climate warming and break-up of ice shelves in the Antarctic Peninsula. Journal of Glaciology 46, 516–530.
Shackleton, N.J., 1987. Oxygen isotopes, ice volume and sea level. Quaternary Science Reviews 6, 183–190.
Sharp, M., Richards, K.S., Arnold, N.S., Lawson, W., Willis, I., Nienow, P., Tison, J.-L., 1993. Geometry, bed topography and drainage system structure of the Haut Glacier d'Arolla, Switzerland. Earth Surface Processes and Landforms 18, 557–571.
Shreve, R.L., 1972. Movement of water in glaciers. Journal of Glaciology 11, 205–214.
Shreve, R.L., 1985. Late wisconsin ice surface profile calculated from esker paths and types, Katahdin Esker System, Maine. Quaternary Research 23, 27–37.
UNESCO, 1970. Climate Atlas of Europe.
Walder, J.S., Fowler, A.C., 1994. Channelized subglacial drainage over a deformable bed. Journal of Glaciology 40, 3–15.